Adsorption, 1, 187–196 (1995)

Predicting Isotherms in Micropores for Different Molecules and Temperatures from a Known Isotherm by Improved Horvath-Kawazoe Equations

LINDA S. CHENG AND RALPH T. YANG*
Department of Chemical Engineering, State University of New York at Buffalo, Buffalo, NY 14260

Abstract. Our improved Horvath-Kawazoe (H-K) equations (by considering the isotherm nonlinearity) for three pore geometries are first summarized. These equations apply to adsorption in microporous materials at subcritical temperatures. From a known isotherm at a given temperature, these equations are used to predict isotherms of the same adsorbate molecules at other temperatures, and also to predict isotherms for other adsorbate molecules at the same (or any subcritical) temperature. A reasonable agreement is obtained between predictions and experimental data. Since the H-K formulation only involves dispersion forces, it underpredicts for gas-solid systems in which other forces also exist. The N_2-zeolite system is one of these systems.

Keywords: micropore size distribution, Horvath-Kawazoe equation, isotherms from pore size distribution

Introduction

Study of equilibrium adsorption in microporous solids, such as carbons, zeolites and pillared clays, is of both fundamental and practical importance. Monte Carlo simulations have been conducted for adsorption in zeolites under supercritical conditions (Soto et al., 1981; Woods and Rowlinson, 1989; Razmus and Hall, 1991). Nitrogen and/or argon adsorption isotherms at subcritical temperatures have been routinely applied to studies of the surface and pore structures of sorbents (Gregg and Sing, 1982). Starting from ultramicropores, adsorption progresses by pore filling as the pressure is increased. For mesopores (20–500 Å), the Kelvin equation, which considers capillary condensation, is applicable for calculating the corresponding pore sizes. On the other hand, for ultramicropores where pore sizes approach a few molecular dimensions, the potential energy fields from neighboring surfaces overlap and the total interaction energy with the adsorbate molecules is substantially enhanced. Here, Kelvin equation is no longer valid.

A theoretical framework combining the microscopic and macroscopic formulation was developed by Horvath and Kawazoe (1983) (H-K) for calculating micropore size distribution of carbon molecular sieve from nitrogen isotherm at the liquid nitrogen temperature. Although simple, it catches the essential feature of progressive pore filling. The H-K model provides a one-to-one correspondence between the pore sizes and the relative pressure at which the pore is filled. It has since been widely applied for micropore size distribution analysis of zeolites (e.g., Venero and Chiou, 1988; Davis et al., 1989; Beck et al., 1992).

Extension of the slit-pore H-K model to cylindrical and spherical pores models has been made (Saito and Foley, 1991; Baksh and Yang, 1991; Cheng and Yang, 1994) considering the curvature effects of pore walls. Recently, Kaminsky et al. (1994) made an assessment of the mean-field methods approach used in H-K model.

Improvement of the H-K formulation has also been made by taking into consideration of the nonlinearity of the adsorption isotherm (Cheng and Yang, 1994), resulting in significant improvements while still preserving the simplicity of the calculation. The experimental measurements of isotherms on microporous sorbents at subcritical temperatures are difficult due to slow diffusion and very low relative pressures needed (e.g., 10^{-7} to 10^{-4}).

The goal of this work is to explore the possibility of applying our improved H-K formulations to derive isotherms at other temperatures and also of other molecules at subcritical temperatures.

Theoretical

(1) *Improved Horvath-Kawazoe Equations for Three Pore Geometries*

Details of the derivation are available elsewhere (Cheng and Yang, 1994). The following is a brief summary.

*Address correspondence to R.T. Yang.

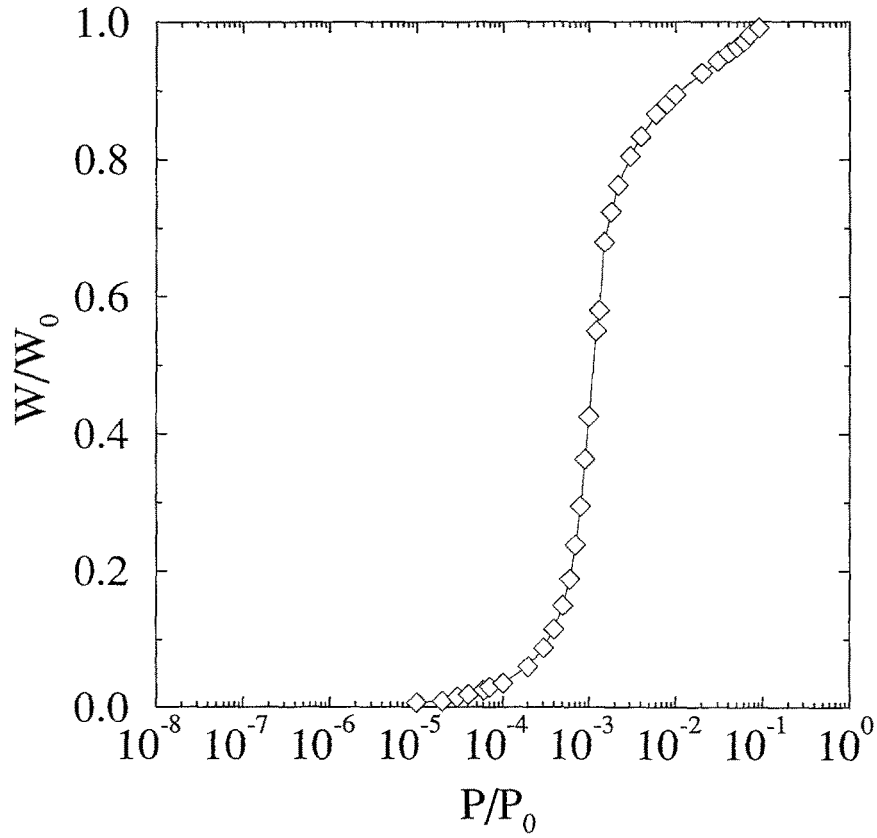

Fig. 1. Adsorption isotherm of argon on Faujasite zeolite at 87 K (Borghard et al., 1991).

Based on Lennard-Jones potential for the dispersion and repulsion energy for adsorbate-adsorbent and adsorbate-adsorbate interactions, Everett and Powl (1976) derived the potential energy of interaction for slit and cylindrical pores as:

For slit pores:

$$\varepsilon(z) = K\varepsilon^*\left[-\left(\frac{\sigma}{z}\right)^4 + \left(\frac{\sigma}{z}\right)^{10} - \left(\frac{\sigma}{L-z}\right)^4 + \left(\frac{\sigma}{L-z}\right)^{10}\right] \quad (1)$$

For cylindrical pores:

$$\varepsilon(r) = \frac{5}{2}\pi\varepsilon^*\left[\frac{21}{32}\left(\frac{d_0}{L}\right)^{10}\sum_{k=0}^{\infty}\alpha_k\left(\frac{r}{L}\right)^{2k} - \left(\frac{d_0}{L}\right)^4\sum_{k=0}^{\infty}\beta_k\left(\frac{r}{L}\right)^{2k}\right] \quad (2)$$

Where constants α_k and β_k are:

$$\alpha_k^{1/2} = \frac{\Gamma(-4.5)}{\Gamma(-4.5-k)\Gamma(k+1)} \quad (3)$$

$$\beta_k^{1/2} = \frac{\Gamma(-1.5)}{\Gamma(-1.5-k)\Gamma(k+1)} \quad (4)$$

Walker (1966) and Soto et al. (1979) showed the following expression of potential energy for the spherical model when considering a zeolite cavity:

$$\Gamma_{1,\mathrm{slp}}(z) = 2N_1\varepsilon_{12}^* \times\left[-\left(\frac{d_0}{L}\right)^6\frac{1}{4\left(\frac{z}{L}\right)}\left(\frac{1}{\left(1-\frac{z}{L}\right)^4} - \frac{1}{\left(1+\frac{z}{L}\right)^4}\right) + \left(\frac{d_0}{L}\right)^{12}\frac{1}{10\left(\frac{z}{L}\right)}\left(\frac{1}{\left(1-\frac{z}{L}\right)^{10}} - \frac{1}{\left(1+\frac{z}{L}\right)^{10}}\right)\right] \quad (5)$$

where

$$N_1 = 4\pi L^2 N_a \quad (6)$$

Horvath and Kawazoe (1983) related the average potential energy to the free energy change upon

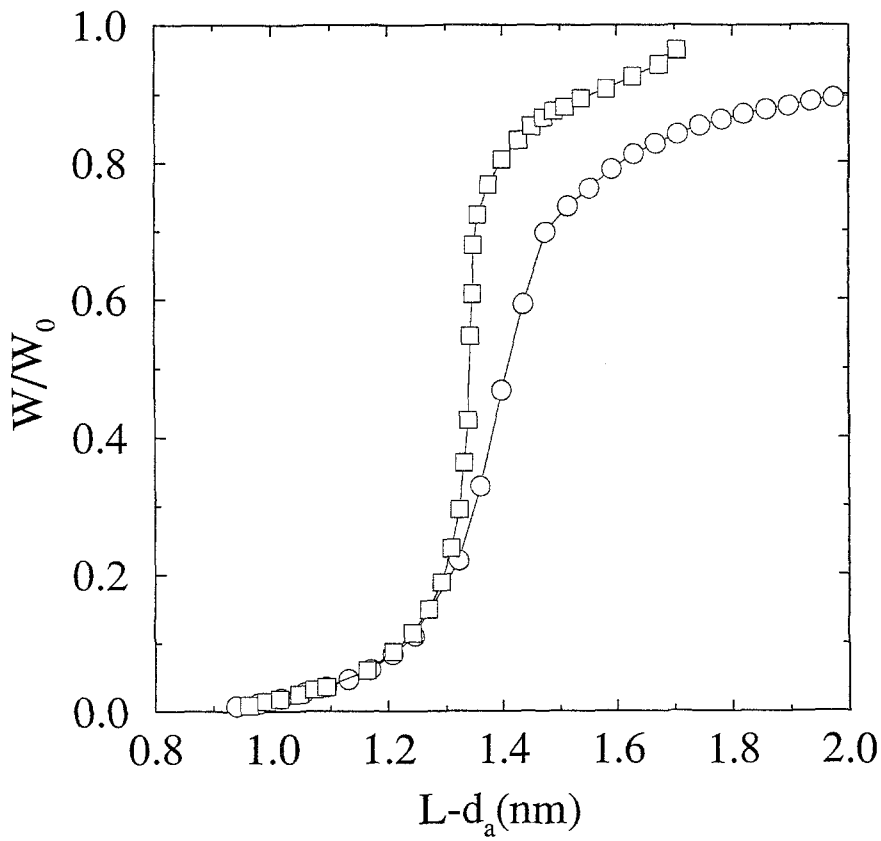

Fig. 2. Effective pore size distribution L-d_a of Faujasite zeolite calculated from (○) original H-K formulation and (□) improved H-K formulation.

adsorption, and obtained for slit pore size distribution:

$$RT\ln\left(\frac{P}{P_0}\right) = N_{AV}\frac{N_aA_a + N_AA_A}{\sigma^4(L-2d_0)}\left[\frac{\sigma^4}{3(L-d_0)^3} - \frac{\sigma^{10}}{9(L-d_0)^9} - \frac{\sigma^4}{3d_0^3} + \frac{\sigma^{10}}{9d_0^9}\right] \quad (7)$$

Taking into account the curvature effect, Saito and Foley (1991) proposed the following for cylindrical pore distribution:

$$RT\ln\left(\frac{P}{P_0}\right) = \frac{3}{4}\pi N_{AV}\frac{N_aA_a + N_AA_A}{d_0^4} \times \sum_{k=0}^{\infty}\left[\frac{1}{(k+1)}\left(1-\frac{d_0}{L}\right)^{2k} \times \left(\frac{21}{32}\alpha_k\left(\frac{d_0}{L}\right)^{10} - \beta_k\left(\frac{d_0}{L}\right)^4\right)\right] \quad (8)$$

Considering adsorption inside a zeolite cavity, we developed the following spherical pore size distribution model (Cheng and Yang, 1994).

$$RT\ln\left(\frac{P}{P_0}\right) = \frac{6(N_1\varepsilon_{12}^* + N_2\varepsilon_{22}^*)L^3}{(L-d_0)^3} \times \left[-\left(\frac{d_0}{L}\right)^6\left(\frac{1}{12}T_1 + \frac{1}{8}T_2\right) + \left(\frac{d_0}{L}\right)^{12}\left(\frac{1}{90}T_3 + \frac{1}{80}T_4\right)\right] \quad (9)$$

where T_1–T_4 are as follows:

$$T_1 = \frac{1}{\left(1-\frac{L-d_0}{L}\right)^3} - \frac{1}{\left(1+\frac{L-d_0}{L}\right)^3}$$

$$T_2 = \frac{1}{\left(1+\frac{L-d_0}{L}\right)^2} - \frac{1}{\left(1-\frac{L-d_0}{L}\right)^2}$$

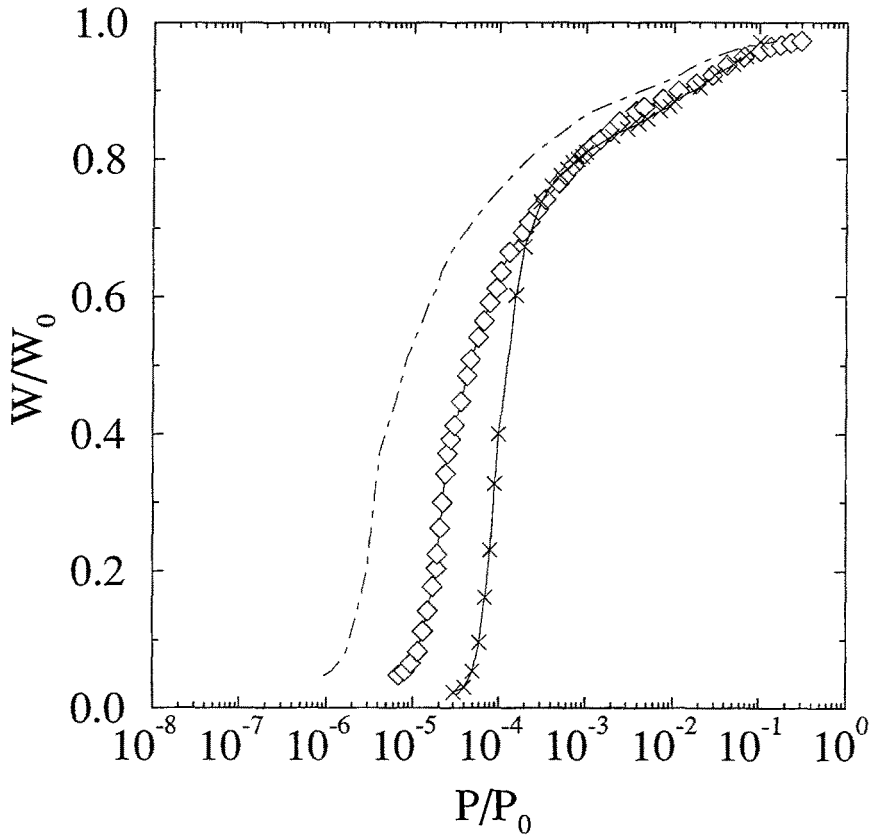

Fig. 3. Adsorption isotherms of argon on $AlPO_4$-11 at 87 K and 77 K. (◇) Experimental data at 87 K. (×) Experimental data at 77 K. (———) Prediction at 77 K.

$$T_3 = \frac{1}{\left(1 - \frac{L-d_0}{L}\right)^9} - \frac{1}{\left(1 + \frac{L-d_0}{L}\right)^9}$$

$$T_4 = \frac{1}{\left(1 + \frac{L-d_0}{L}\right)^8} - \frac{1}{\left(1 - \frac{L-d_0}{L}\right)^8}$$

All the above models are based on the Horvath-Kawazoe assumption of Henry's Law region adsorption:

$$\Pi = \frac{kT}{\beta}\theta \tag{10}$$

However, the isotherms for adsorption in micropores under subcritical conditions (e.g., N_2 at 77 K and Ar at 87 K) follow the typical Type I behavior (Gregg and Sing, 1982). Consequently we replace the equation of state for two-dimensional ideal gas with the Langmuir-type equation of state:

$$\Pi = \frac{kT}{\beta} \ln \frac{1}{1-\theta} \tag{11}$$

We, then, arrived at our improved H-K equations for slit, cylindrical and spherical pore geometries as follows:

Slit-Shaped Pore:

$$RT \ln\left(\frac{P}{P_0}\right) + \left[RT - \frac{RT}{\theta} \ln \frac{1}{1-\theta}\right]$$

$$= N_A \frac{N_a A_a + N_A A_A}{\sigma^4 (L - 2d_0)}$$

$$\times \left[\frac{\sigma^4}{3(L-d_0)^3} - \frac{\sigma^{10}}{9(L-d_0)^9} - \frac{\sigma^4}{3d_0^3} + \frac{\sigma^{10}}{9d_0^9}\right] \tag{12}$$

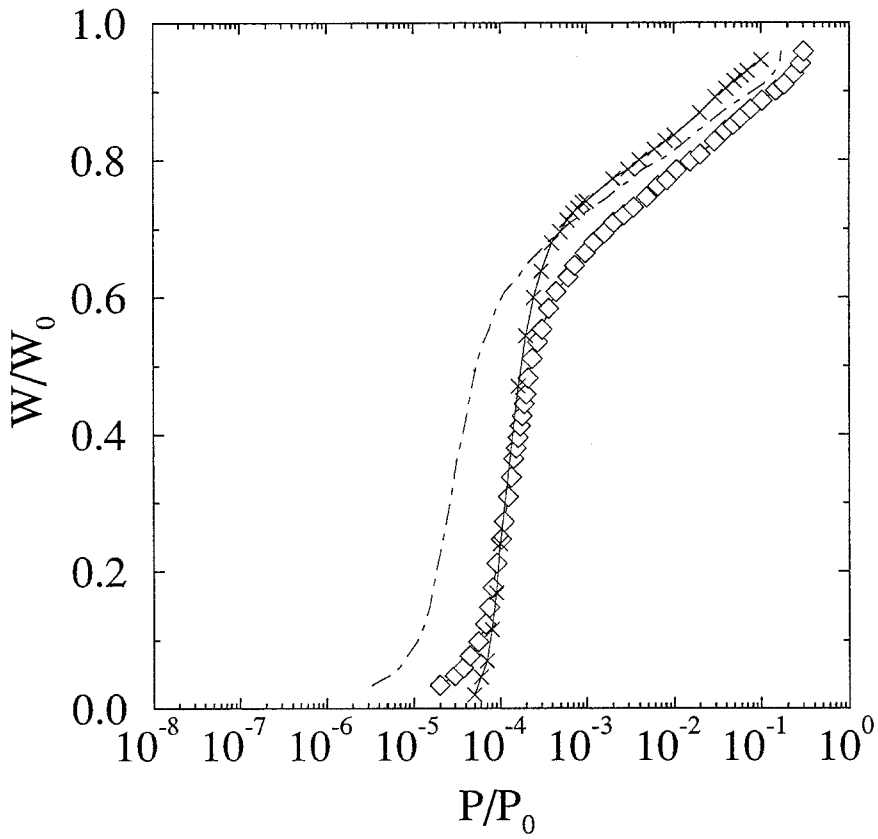

Fig. 4. Adsorption isotherms of argon on $AlPO_4$-5 at 87 K and 77 K. (◇) Experimental data at 87 K. (×) Experimental data at 77 K. (—·—·—) Prediction at 77 K.

Cylindrical Pore:

$$RT\ln\left(\frac{P}{P_0}\right)+\left[RT-\frac{RT}{\theta}\ln\frac{1}{1-\theta}\right] = \frac{3}{4}\pi N_{AV}\frac{N_aA_a+N_AA_A}{d_0^4}\sum_{k=0}^{\infty}\left[\frac{1}{(k+1)} \times\left(1-\frac{d_0}{L}\right)^{2k}\left(\frac{21}{32}\alpha_k\left(\frac{d_0}{L}\right)^{10}-\beta_k\left(\frac{d_0}{L}\right)^4\right)\right] \tag{13}$$

Spherical Pore:

$$RT\ln\left(\frac{P}{P_0}\right)+\left[RT-\frac{RT}{\theta}\ln\frac{1}{1-\theta}\right] = \frac{6\left(N_1\varepsilon_{12}^*+N_2\varepsilon_{22}^*\right)L^3}{(L-d_0)^3} \times\left[-\left(\frac{d_0}{L}\right)^6\left(\frac{1}{12}T_1+\frac{1}{8}T_2\right)+\left(\frac{d_0}{L}\right)^{12}\left(\frac{1}{90}T_3+\frac{1}{80}T_4\right)\right] \tag{14}$$

where T_1–T_4 are given in the foregoing.

(2) *Predicting Isotherms by Improved H-K Equations*

As have been stated, the H-K formalism renders a one-to-one correspondence between the pore size and the relative pressure at which the pore is filled. Therefore, from the isotherm $W/W_0 = q(P/P_0)$, the relation $W/W_0 = f(L-d_a)$ (where $L-d_a$ is the effective pore dimension) can be established, and thus the pore size distribution. Now that we have obtained the pore size distribution, we can go through a reverse

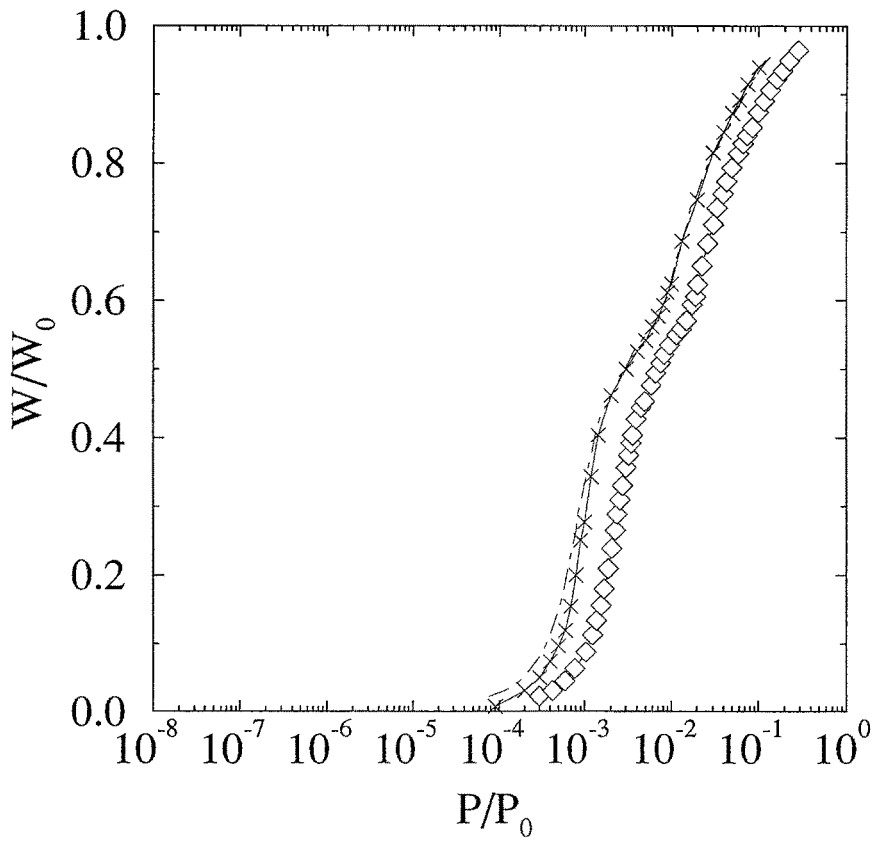

Fig. 5. Adsorption isotherms of argon on VPI-5 at 87 K and 77 K. (◊) Experimental data at 87 K. (×) Experimental data at 77 K. (——) prediction at 77 K.

Table 1. Physical parameters of nitrogen and oxygen.

	Adsorbate	
Parameter	Oxygen	Nitrogen
Diameter, d, nm	0.346[a]	0.364[a]
Polarizability, α, cm^3	1.57×1^{-24}[b]	1.74×10^{-24}[c]
Magnetic susceptibility, χ, cm^3	1.52×10^{-29}[b]	2.0×10^{-29}[d]
Density, N, molecule/cm^2	7.76×10^{14}[e]	6.71×10^{14}[e]

[a] Breck (1974).
[b] Steele (1974).
[c] Venero and Chiou (1986).
[d] Horvath and Kawazoe (1983).
[e] Estimated from Handbook of Chemistry and Physics by Weast (1987).

procedure to calculate other isotherms provided appropriate physical parameters are known. In this manner we can predict isotherms at other subcritical temperatures as well as for other molecules.

The adsorbent physical parameter used in this work can be found in Cheng and Yang (1994) while the adsorbate physical parameters are listed in Table 1.

Results and Discussion

(1) Comparison of H-K and Improved H-K Formulations

At 87 K, Ar adsorption in faujasite, like in all other microporous materials, has a characteristic sigmoidal shape as shown in semi-log form in Fig. 1.

The cumulative pore size distribution of faujasite calculated from both spherical models of Eqs. (9) and (14) are shown in Fig. 2. The broad pore size distribution pattern calculated from the original H-K formulation, Eq. (9), apparently does not reflect the crystalline nature of zeolite. One reason is that the original H-K

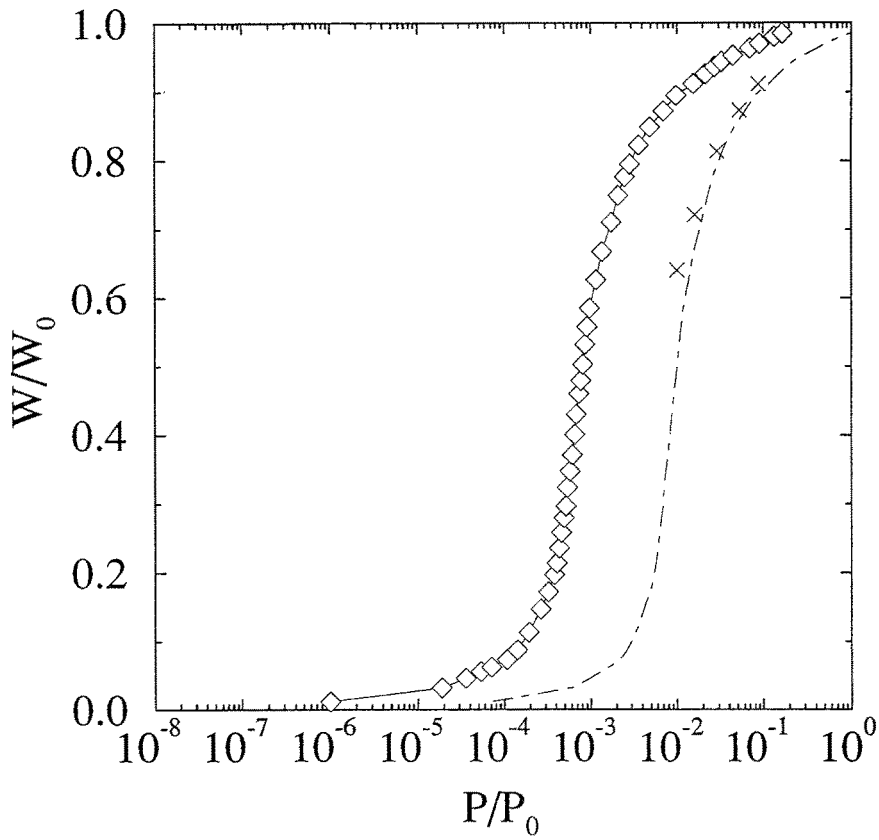

Fig. 6. Adsorption isotherms of Ar at 87 K and Oxygen at 90 K on Y zeolite. (◇) Experimental data of Ar at 87 K. (×) Experimental data of O_2 at 90 K. (—·—) Prediction of O_2 at 90 K.

formulation assumes the linear isotherm (i.e., Henry's Law Region). In our study the nonlinearity of the isotherm (i.e., Langmuir Equation) is taken into consideration, which results in the coverage (θ)-dependent term: $RT - \frac{RT}{\theta} \ln \frac{1}{1-\theta}$. A significant difference is observed when applying the improved H-K formulation, Eq. (14). The pore size distribution becomes sharper, indicating more uniform pores characteristic of zeolitic materials.

The integral molar enthalpy change of adsorption is expressed as:

$$\Delta H^{\text{ads}} = -q^{\text{diff}} - RT + \left(\frac{T\beta}{\theta}\right)\left(\frac{\partial \Pi}{\partial T}\right)_{\theta} \quad (15)$$

or

$$\Delta H^{\text{ads}} = -q^{\text{st}} + T\left(S^s - \bar{S}^s\right) \quad (16)$$

In the original H-K formulation, $S^s - \bar{S}^s$ is assumed to be equal to the gas constant, R, throughout the entire range of coverage. However, such an assumption is valid only for a two-dimensional ideal gas or when θ approaches zero. As shown in Fig. 1, the transition pressure for microporous adsorption (i.e., the initial inflection point) occurs when θ approaches 0.5. Consequently, the Henry's Law assumption is no longer valid. With the Langmuir equation of state, the dependence of ΔH^{ads} on the degree of filling, θ, is taken into consideration, which results in a better pore size distribution, and the peak pore size of 13.5 Å compares well with the literature (Uppal, 1988).

(2) *Temperature Dependence of Adsorption Isotherm*

Experimental adsorption isotherm of Ar at 87 K on the aluminophosphate molecular sieves $AlPO_4$-11, $AlPO_4$-5 and VPI-5 taken from Hathaway et al. (1990) are shown in Figs. 3–5. Since all of the above microporous materials consist of one dimensional channels, the cylindrical pore model, Eq. (13), is used. The predicted isotherm along with the experimental isotherm

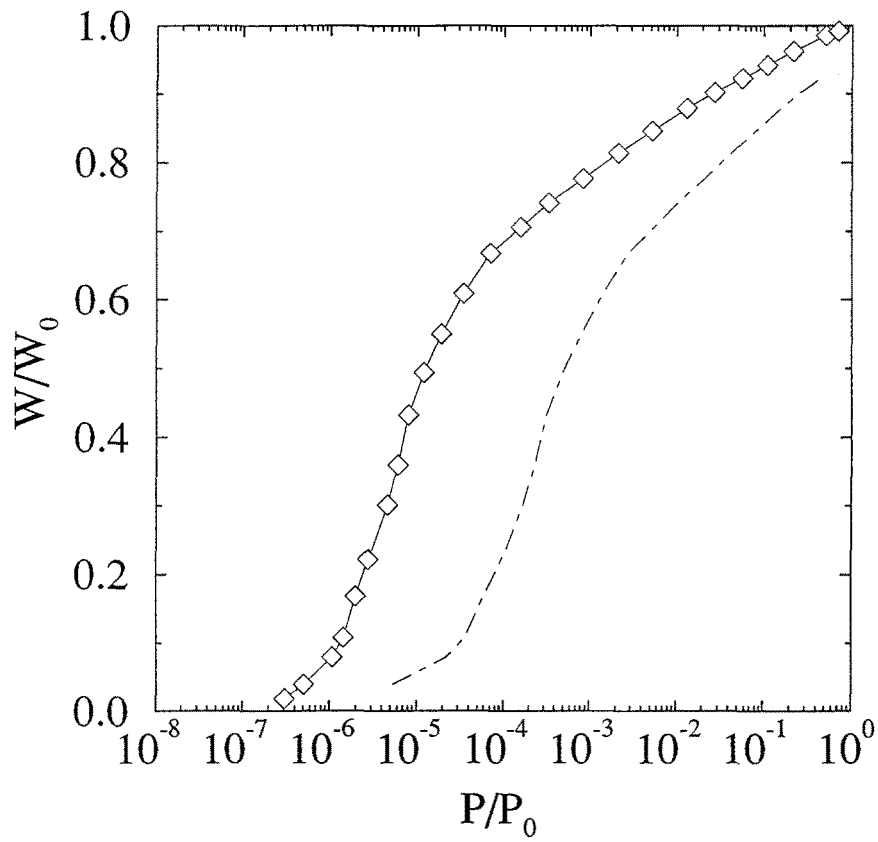

Fig. 7. Adsorption isotherms of N_2 at 77 K and oxygen at 90 K on carbon molecular sieve HGS 638. (◊) Experimental data at N_2 at 77 K. (—·—) Prediction of O_2 at 90 K.

taken from the same source as above for Ar at 77 K are also presented in these figures. The pore dimensions of these three molecular sieves follow the sequence:

$$\text{Al PO}_4\text{-11}(6.3 \times 3.9\ \text{Å}) < \text{Al PO}_4\text{-5}(7.3\ \text{Å}) < \text{VPI-5}(12.1\ \text{Å})$$

As shown in Figs. 3–5, the agreement between the predictions and the experimental isotherms diminishes as the pore size gets smaller. Two possible factors contribute to the disagreement. At lower temperatures, diffusion becomes slower and longer times are needed for the experiment to reach equilibrium. The quasi-equilibrium conditions used by Hathaway et al. (1990) may not have allowed the system to reach equilibrium as compared to static-equilibrium conditions, thus resulting in a shift of isotherm towards a higher pressure.

Saito and Foley (1991) and Lastoskie et al. (1993) have also made the point that the static technique is required especially in low pressure ranges where ultramicropore adsorption takes place, in order to reach a near equilibrium state during the uptake. Another source of discrepancy is that the H-K formulations are based on a continuum approach. This approach breaks down when the pores are very small and the number of layers of adsorbate becomes very few.

(3) Oxygen and Nitrogen Isotherms

Based on Venero and Chiou's data (1988) of Ar isotherm on Y zeolite, we calculated the oxygen isotherm at 90 K using the spherical pore model, Eq. (14). Along with experimental points for the same system from Breck (1983), the isotherms are shown in Fig. 6. Breck's data at very low pressures were not taken at equilibrium and are hence not included. The experimental adsorption points of O_2 adsorption at 90 K are in good agreement with the predicted isotherm.

Horvath and Kawazoe (1983) reported data on N_2 on a carbon molecular sieve (HGS 683) at 77 K. The improved slit-pore model, Eq. (12), is used to predict

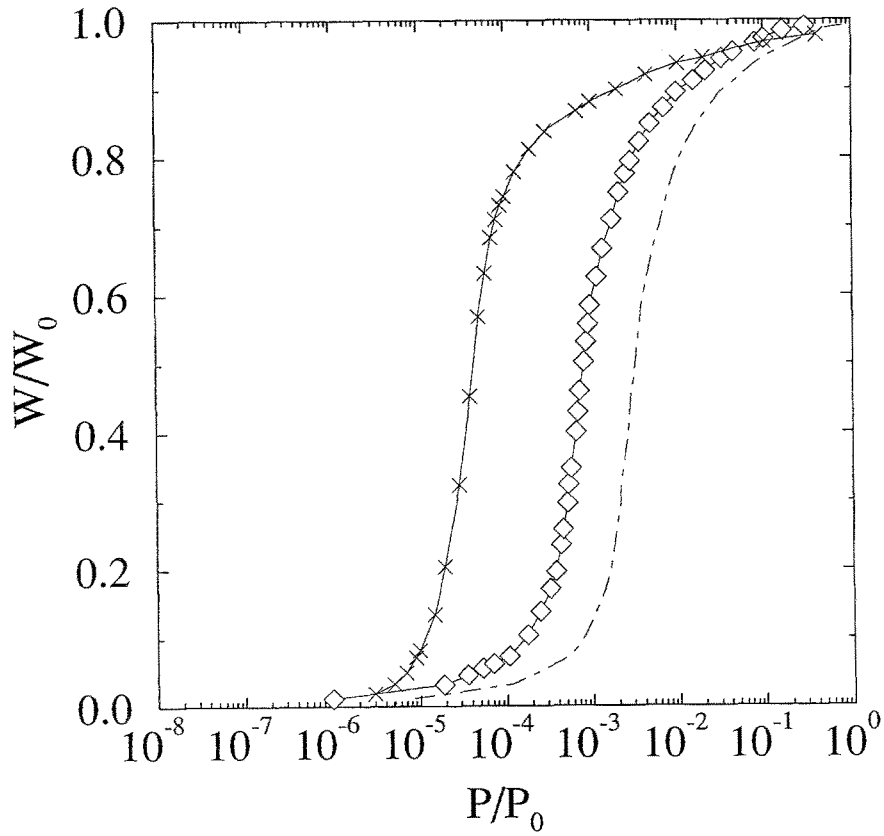

Fig. 8. Adsorption isotherms of N_2 at 77 K on Y zeolite. (◊) Experimental data of Ar at 87 K. (×) Experimental data of N_2 at 77 K. (——) Prediction of N_2 at 77 K based on Ar data.

O_2 isotherm at 90 K on the same sorbent, shown along with the N_2 isotherm in Fig. 7. No experimental data, however, for O_2 isotherm is available for comparison with the prediction.

The nitrogen isotherm on Y zeolite at 77 K is also predicted and shown in Fig. 8, together with the experimental result of Venero and Chiou (1988). Clearly the model fails to predict the nitrogen isotherm. The predicted isotherm appears at a higher relative pressure than the experimental data. This can be attributed to the fact that the H-K model only considers dispersion repulsion interaction forces while electrostatic forces are not included. As a result, for weakly quadrupolar and non-polar and non-quadrupolar molecules, such as argon and oxygen, the prediction is in good agreement with the experimental data. Nitrogen has a strong quadrupole moment, which causes electrostatic forces. Thus the prediction underestimates the isotherm. The additional electrostatic forces for N_2 shift the isotherm toward a smaller P/P_0 value for the pore dimension. Further work is needed to include the electrostatic forces in the H-K model.

Nomenclature

A	dispersion constant
c	speed of light
d	diameter of atom
d_0	arithmetic mean of diameters of adsorbate and adsorbent atoms
H^{ads}	enthalpy of adsorption
k	Boltzmann constant
L	distance between nuclei of the parallel layers for slit-shaped pores, likewise defined as the radius (not diameter) for cylindrical and spherical pores
N	density per unit area
N_{AV}	Avogadro's number
P	pressure

P_0	saturate vapor pressure of adsorbate
q^{diff}	differential heat of adsorption
q^{st}	isosteric heat of adsorption
r	distance between gas molecule and cylinder's central axis (cylindrical model) or gas molecule and oxygen atom in the spherical wall (spherical model)
R	gas constant
S^s	molar entropy of adsorbate
$\bar{S}^s$	differential molar entropy of adsorbate
T	absolute temperature
W	amount adsorbed
W_0	saturated amount adsorbed
z	distance of adsorbate molecule from a surface atom in the slit layer for slit pore model or from the cavity center for spherical pore model

Greek Letters

α	polarizability
α_k	constant, Eq. (3)
β	molecular area (area/adsorbate molecular)
β_k	constant, Eq. (4)
χ	magnetic susceptibility
ε	potential energy of interaction
σ	distance from an atom in the surface layer at zero interaction energy
Γ	potential energy of interaction in zeolite cavity
θ	degree of void filling, or angle in spherical coordinate system, $0 \leq \theta \leq \pi$, in Eq. (10)
Π	spreading pressure

Subscripts

1	adsorbent atom
2	adsorbate molecule (or atom)
a	adsorbent
A	adsorbate

Acknowledgment

The work was supported by NSF under grant CTS-9212279.

References

Baksh, M.S.A. and R.T. Yang, "Model for spherical cavity radii and potential functions of sorbated in zeolites," *AIChE J.*, **37**, 923 (1991).

Beck, J.S., J.C. Vartuli, W.J. Roth, M.E. Leonowicz, C.T. Kresge, K.D. Schmitt, C.T.-W. Chu, D.H. Olson, E.W. Sheppard, S.B. McCullen, J.B. Higgins, and J.L. Schlenker, "A new family of mesoporous molecular sieves prepared with liquid crystal templates," *J. Am. Chem. Soc.*, **114**, 10835 (1992).

Borghard, W.S., E.W. Sheppard, and H.J. Schoennagel, "An automated, high precision unit for low-pressure physisorption," *Rev. Sci. Instrum.*, **62**(11), 2801 (1991).

Breck, D.W., *Zeolite Molecular Sieves: Structure, Chemistry, and Use*, John Wiley & Sons, New York, 1974.

Cheng, L.S. and R.T. Yang, "Improved Horvath-Kawazoe Equations Including Spherical Pore Models for Calculating Micropore Size Distribution," *Chem. Eng. Sci.*, **49**, 2599 (1994).

Davis, M.E., C. Montes, P.E. Hathaway, J.P. Arhancet, D.L. Hasha, and J.E. Garces, "Physicochemical properties of VPI-5," *J. Am. Chem. Soc.*, **111**, 3919 (1989).

Everett, D.H. and J.C. Powl, "Adsorption in slit-like cylindrical micropores in the Henry's law region," *J. Chem. Soc. Faraday Trans. 1*, **72**, 619 (1976).

Gregg, S.J. and K.S.W. Sing, *Adsorption, Surface Area and Porosity*, Academic Press, London, 1982.

Hathaway, P.E. and M.E. Davis, "High resolution, quasi-equilibrium sorption studies of molecular sieves," *Catal. Lett.*, **5**, 333 (1990).

Horvath, G. and K. Kawazoe, "Method for calculation of effective pore size distribution in molecular sieve carbon," *J. Chem. Eng. Japan*, **16**, 470 (1983).

Kaminsky, R.D., Maglara, E., and Conner, W.C., "A Direct Assessment of Mean-Field Methods of Determining Pore Size Distributions of Microporous Media from Adsorption Isotherm Data," *Langmuir*, **10**, 1556 (1994).

Lastoskie, C., K.E. Gubbins, and N. Quirke, "Pore size distribution analysis of microporous carbons: A density functional theory approach," *J. Phys. Chem.*, **97**, 4786 (1993).

Razmus, D.M. and C.K. Hall, "Prediction of Gas Adsorption in 5A Zeolites Using Monte Carlo Simulation," *AIChE J.*, **37**(5), 769 (1991).

Saito, A. and H.C. Foley, "Curvature and parametric sensitivity in models for adsorption in micropores," *AIChE J.*, **37**(3), 429 (1991).

Soto, L.J, P.W. Fisher, A.J. Glessner, and A.L. Myers, "Sorption of gases in molecular sieves-theory for Henry's constant," *J. Chem. Soc. Farad. Trans. I*, **77**, 157 (1981).

Steele, W.A., *The Interaction of Gases With Solid Surfaces*, Pergamon Press, New York 1974.

Uppal, M.K., O. Terasaki, and J.M. Thomas, "Optimal conditions for imaging silver cations in zeolite Y," *Zeolites*, **8**, 393 (1988).

Venero, A.F. and J.N. Chiou, "Characterization of zeolites by gas adsorption at low pressures," *MRS Symp. Proc.*, **111**, 235 (1988).

Walker, P.L., *Chemistry and Physics of Carbon*, **2**, Dekker, New York, 1966.

Weast, R.C., *Handbook of Chemistry and Physics*, CRC Press, Boca Raton, Florida, 1987.

Woods, G.B. and J.S. Rowlinson, "Computer Simulations of Fluids in Zeolites X and Y," *J. Chem. Soc. Faraday Trans. 2*, **85**(6), 765 (1989).